nature astronomy

Supplementary information

https://doi.org/10.1038/s41550-026-02795-9

An adolescent and near-resonant planetary system near the end of photoevaporation

In the format provided by the authors and unedited

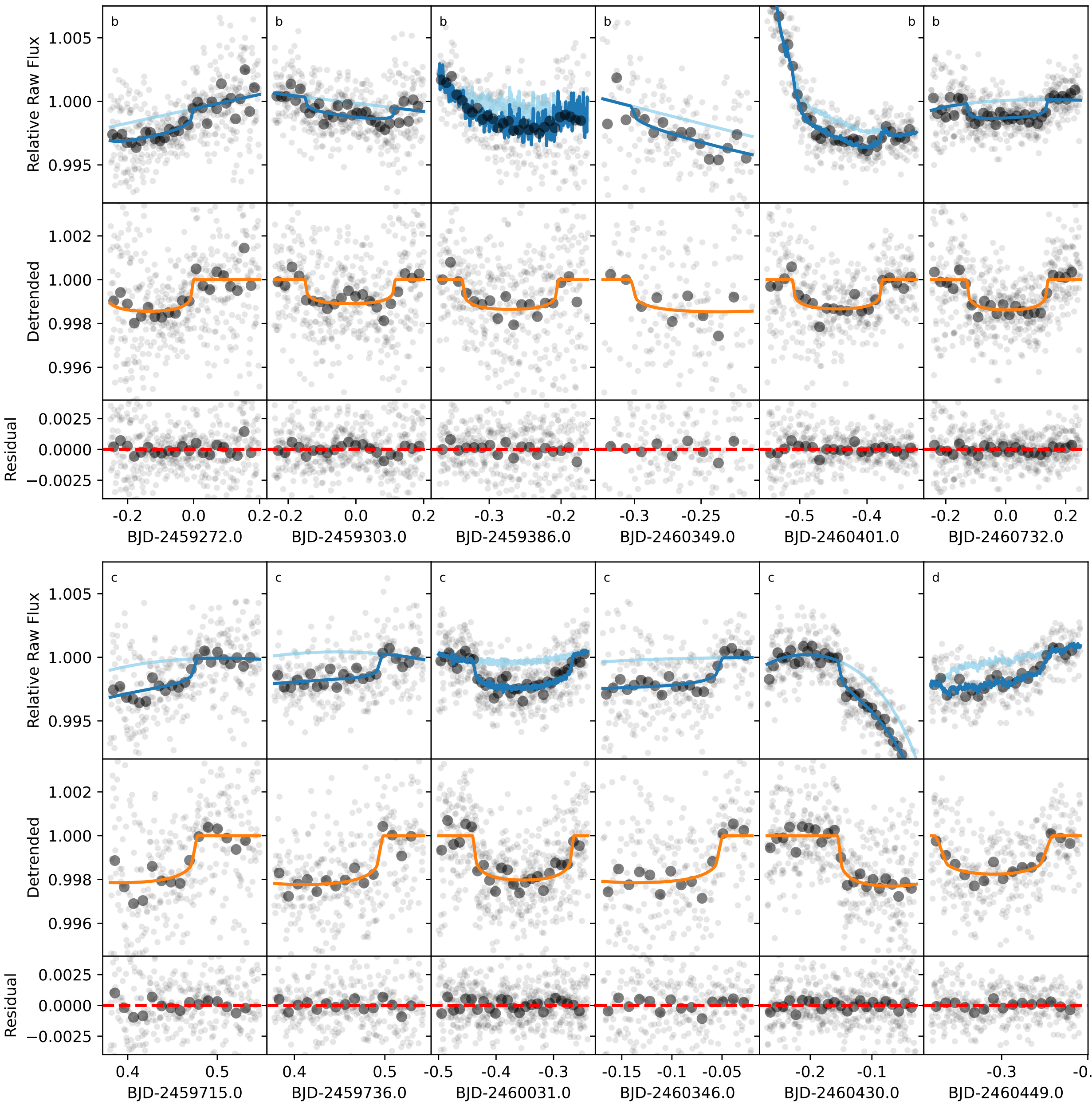

Supplementary Figue 1: **LCO light curves of TOI-2076 planets.** The LCO z_s band light curves of TOI-2076 bcd planets. For each panel, the top row shows the raw fluxes (gray dots) and fluxes binned to 10 minutes (black dots), with the relevant planet index shown on top left. Blue lines are transit models with systematic-induced trends and light blue lines show the trends separately. Middle rows shows detrended light curves with best-fit transit model (orange), and bottom row shows light curve residuals.

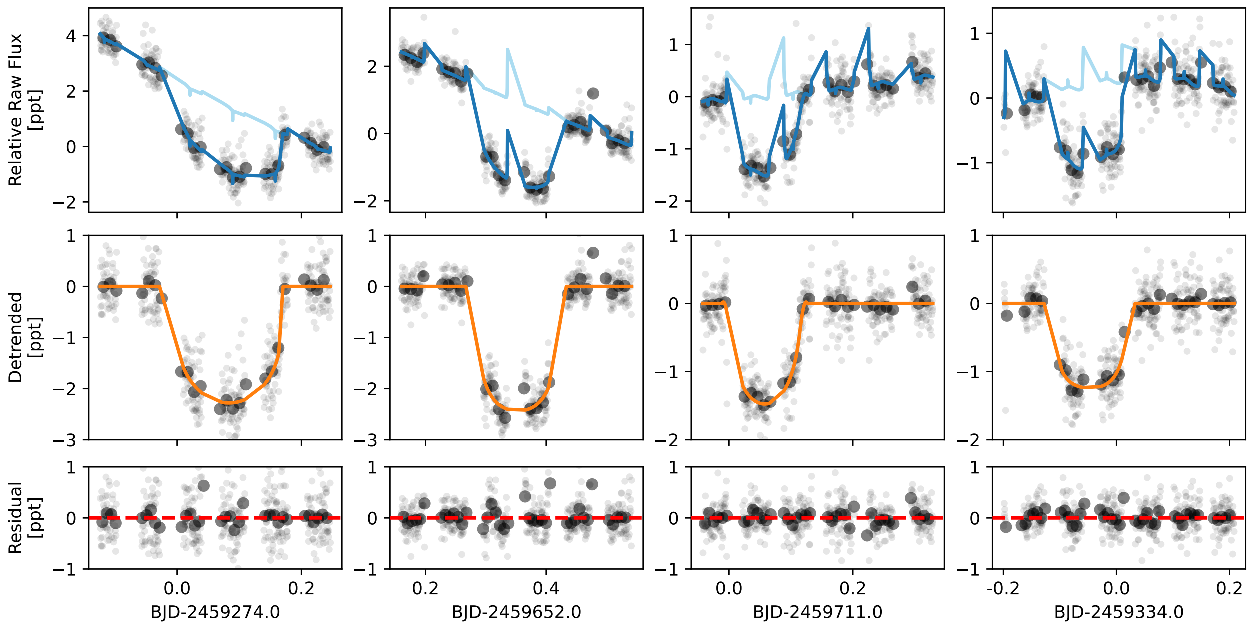

Supplementary Figue 2: **CHEOPS light curves of TOI-2076 planets.** Annotations are the same as Figure 1.

Supplementary Table 1: **Overview of LCO observations**.LCO-McD: McDonald Observatory, Texas, United States (McD); LCO-TEID: Teide Observatory, Tenerife (TEID)

Instrument	Start Date (UTC)	End Date (UTC)	Band	N_{Exp}	Planet	Type
LCO-McD	2021-02-26 06:33:53	2021-02-26 11:59:40	z_s	429	b	Full
LCO-McD	2021-03-29 06:42:47	2021-03-29 11:59:59	z_s	425	b	Full
LCO-McD	2021-06-20 03:06:34	2021-06-20 08:05:49	z_s	392	b	Full
LCO-Teid	2024-02-08 04:13:49	2024-02-08 06:55:12	z_s	176	b	Ingress
LCO-Teid	2024-03-30 22:49:57	2024-03-31 04:09:38	z_s	405	b	Full
LCO-McD	2025-02-25 06:37:09	2025-02-25 12:35:37	z_s	483	b	Full
LCO-Teid	2022-05-15 21:07:50	2022-05-16 01:07:49	z_s	317	c	Egress
LCO-Teid	2022-06-05 21:04:14	2022-06-06 01:01:47	z_s	322	c	Egress
LCO-Teid	2023-03-27 00:00:10	2023-03-27 06:14:00	z_s	497	c	Full
LCO-McD	2024-02-05 07:56:48	2024-02-05 11:31:15	z_s	270	c	Egress
LCO-McD	2024-04-29 05:31:00	2024-04-29 11:19:53	z_s	435	c	Ingress
LCO-McD	2024-05-18 02:50:21	2024-05-18 06:59:52	z_s	337	d	Full

Supplementary Table 2: **Observed transit epochs and midtimes for all three planets in TOI-2076.** a: excluded from TTV analysis.

Epoch	Transit Midtime (BJD-2457000)	Uncertainty (days)	Instrument
planet e			
0	1737.180700	0.0032	TESS
1	1740.203100	0.0009	TESS
2	1743.239800	0.0044	TESS
3	1746.257700	0.0053	TESS
4	1749.288600	0.0041	TESS
5	1752.297000	0.0050	TESS
6	1755.320600	0.0046	TESS
7	1758.357100	0.0037	TESS
63	1927.600300	0.0075	TESS
64	1930.619500	0.0062	TESS
65	1933.638800	0.0065	TESS
66	1936.667000	0.0049	TESS
68	1942.700100	0.0019	TESS
69	1945.738900	0.0050	TESS
70	1948.755000	0.0044	TESS
71	1951.787200	0.0055	TESS
308	2668.062800	0.0024	TESS
309	2671.096000	0.0039	TESS
310	2674.125300	0.0047	TESS
313	2683.174500	0.0017	TESS
314	2686.203600	0.0052	TESS
548	3393.439400	0.0038	TESS
549	3396.459100	0.0057	TESS
556	3417.610000	0.0038	TESS
557	3420.632000	0.0100	TESS
planet b			
0	1743.7180	0.0037	TESS
1	1754.0776	0.0011	TESS
18	1930.1254	0.0019	TESS
19	1940.4806	0.0024	TESS
20	1950.8339	0.0010	TESS
51	2271.8330	0.0039	LCO
54	2302.8954	0.0056	LCO
57	2333.9544	0.0021	CHEOPS
62	2385.7322	0.0045	LCO
89	2665.3387	0.0016	TESS
90	2675.6944	0.0013	TESS
91	2686.0499	0.0012	TESS
155[a]	3348.7591	0.0078	LCO
160	3400.5577	0.0026	LCO
162	3421.2644	0.0011	TESS
192	3731.9025	0.0018	LCO
planet c			
0	1748.69389	0.00078	TESS
9	1937.82322	0.00086	TESS
25	2274.08475	0.00061	CHEOPS
43	2652.35118	0.00049	CHEOPS
44	2673.36567	0.00067	TESS
46	2715.39312	0.00382	LCO
47	2736.41236	0.00206	LCO
61	3030.64815	0.00136	LCO
76	3345.86622	0.00308	LCO
80	3429.92971	0.00206	LCO
planet d			
0	1762.66666	0.00173	TESS
5	1938.29185	0.00218	TESS
18	2394.92676	0.00120	LCO
26	2675.93174	0.00115	TESS
27	2711.05693	0.00082	CHEOPS
48	3448.69029	0.00191	LCO

Supplementary Table 3: **RV analysis Results with Gaussian Process.** $\mathcal{N}(\mu, \sigma)$ is normal prior with mean value of μ and variance of σ; $\mathcal{J}(a, b)$ is Jeffreys (log-uniform) prior with lower and upper bounds a, b; $\mathcal{U}(a, b)$ is uniform prior with lower and upper bounds a, b.

Parameters	Prior	Posterior
Planet Parameters		
P_b [day]	$\mathcal{N}(10.355230, 1 \times 10^{-5})$	10.35523 ± 0.00001
$T_{\rm b,conj}$ [BJD-2450000]	$\mathcal{N}(8950.8289, 5 \times 10^{-4})$	8950.82890 ± 0.00044
K_b [m/s]	$\mathcal{U}(-50, 50)$	$2.32^{+0.63}_{-0.63}$
P_c [day]	$\mathcal{N}(21.01549, 3 \times 10^{-5})$	21.01549 ± 0.00003
$T_{\rm c,conj}$ [BJD-2450000]	$\mathcal{N}(8937.8283, 7 \times 10^{-4})$	8937.82829 ± 0.00062
K_c [m/s]	$\mathcal{U}(-50, 50)$	$1.78^{+0.63}_{-0.62}$
P_d [day]	$\mathcal{N}(35.12551, 7 \times 10^{-5})$	35.12551 ± 0.00006
$T_{\rm d,conj}$ [BJD-2450000]	$\mathcal{N}(8938.296, 1 \times 10^{-3})$	8938.296008 ± 0.0009
K_d [m/s]	$\mathcal{U}(-50, 50)$	$1.32^{+0.59}_{-0.56}$
P_e [day]	$\mathcal{N}(3.0223445, 3 \times 10^{-5})$	3.02234 ± 0.00003
$T_{\rm e,conj}$ [BJD-2450000]	$\mathcal{N}(8740.21306, 8 \times 10^{-3})$	8740.2127 ± 0.0072
K_e [m/s]	$\mathcal{U}(-50, 50)$	$2.40^{+0.67}_{-0.65}$
GP Parameters		
$h_{\rm RV}$ [m/s]	$\mathcal{J}(0.001, 1000)$	$34.60^{+2.16}_{-1.92}$
τ [day]	$\mathcal{J}(0.001, 1000)$	$26.56^{+1.27}_{-1.18}$
Γ	$\mathcal{J}(0.001, 1000)$	$6.07^{+0.64}_{-0.56}$
$P_{\rm rot}$ [day]	$\mathcal{N}(7.34, 0.2)$	$7.34^{+0.01}_{-0.01}$
Instrumental Parameters		
$\gamma_{\rm HIRES}$ [m/s]	$\mathcal{U}(-50.0, 50.0)$	$0.10^{+4.14}_{-4.22}$
$\gamma_{\rm APF}$ [m/s]	$\mathcal{U}(-50.0, 50.0)$	$-7.34^{+4.35}_{-4.45}$
$\gamma_{\rm HARPS}$ [m/s]	$\mathcal{U}(-50.0, 50.0)$	$5.38^{+3.90}_{-4.11}$
$\sigma_{\rm HIRES}$ [m/s]	$\mathcal{J}(0.001, 1000)$	$8.15^{+1.31}_{-1.15}$
$\sigma_{\rm APF}$ [m/s]	$\mathcal{J}(0.001, 1000)$	$11.74^{+1.78}_{-1.62}$
$\sigma_{\rm HARPS}$ [m/s]	$\mathcal{J}(0.001, 1000)$	$4.69^{+0.82}_{-0.76}$
Derived Masses		
Mass b [$M_\oplus$]		$7.13^{+1.92}_{-1.94}$
Mass c [$M_\oplus$]		$6.91^{+2.45}_{-2.42}$
Mass d [$M_\oplus$]		$6.11^{+2.73}_{-2.57}$
Mass e [$M_\oplus$]		$4.89^{+1.36}_{-1.33}$

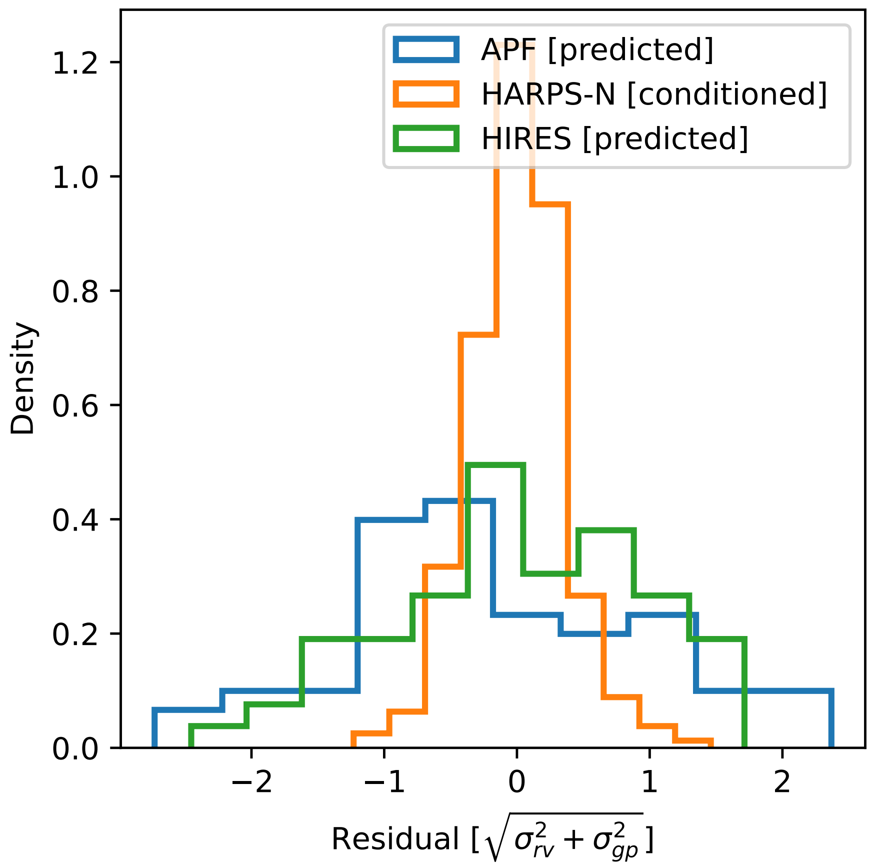

Supplementary Figue 3: **Cross-validation test of GP model.** The best-fit GP model is conditioned on HARPS data and used to predict the contemporaneous HIRES and APF RV data. The histogram shows the residual of the RV data subtracted by GP model, which are given in unit of the quadracture sum of RV measurement error and GP standard deviation.

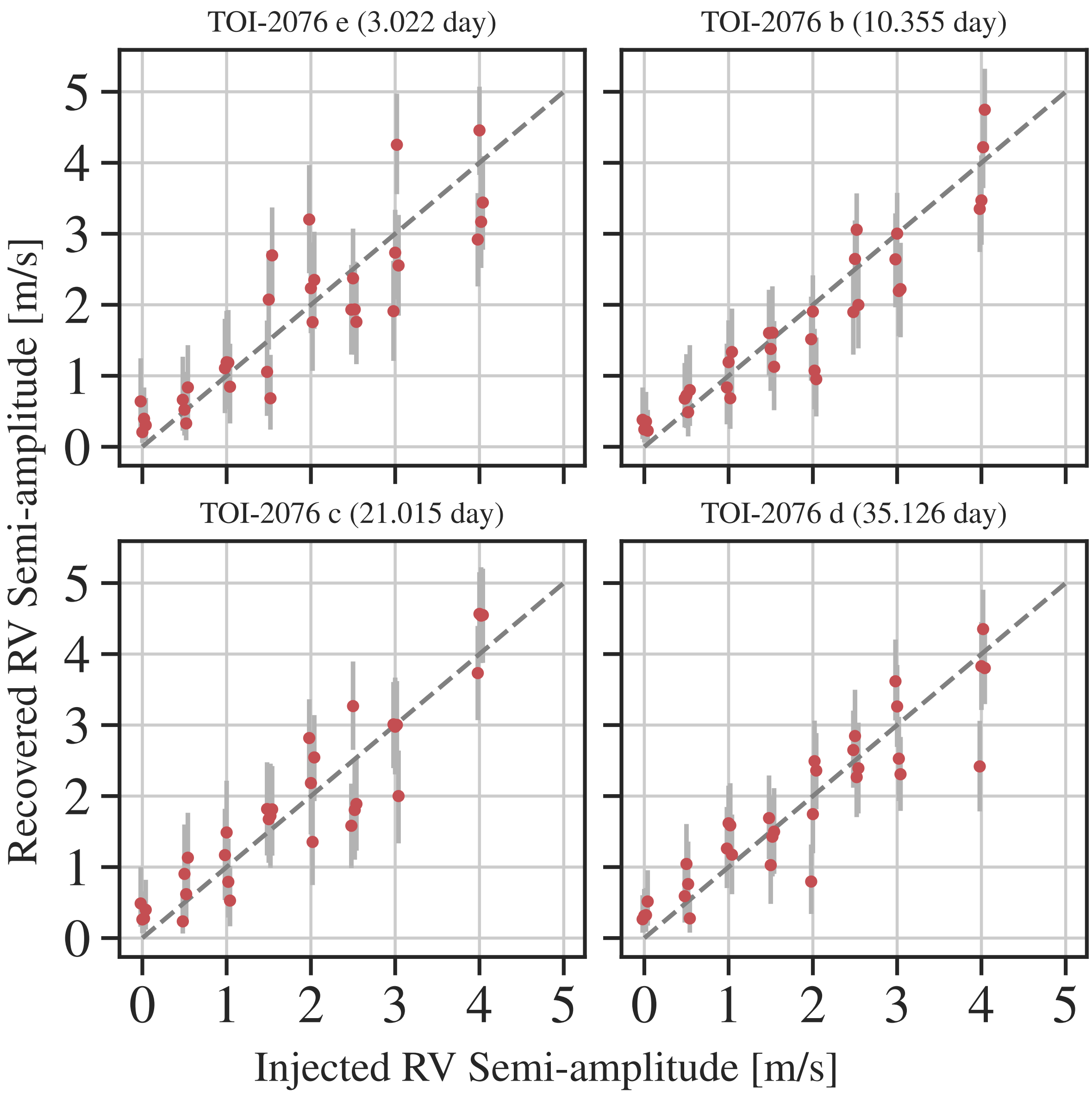

Supplementary Figue 4: **The accuracy of retrieved semi-amplitudes of planetary RV signals from GP model.** The median and 68% credible intervals of the recovered planetary RV semi-amplitudes as a function of the injected semi-amplitudes, based on simulated datasets for the four planets in the system.

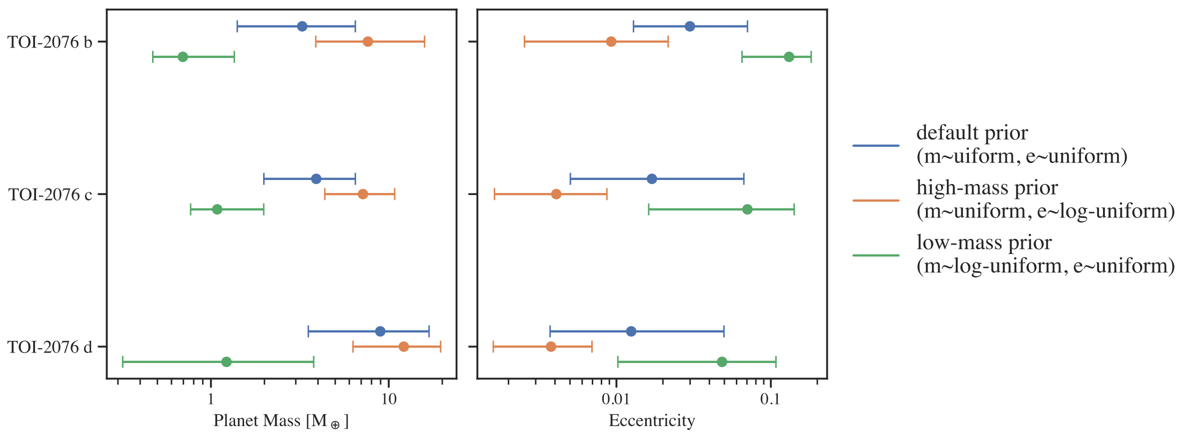

Supplementary Figue 5: **Comparisons of planetary mass and eccentricity from TTV analysis with different priors.** The errorbar shows the median and 68% credible interval of each parameter. These parameters constrained by TTV data alone are highly degenerate and is sensitive to adopted priors.

Supplementary Table 4: **Posterior median and 68.3% (1σ) credible intervals of fitted planetary orbit parameters from the TTV-only model and joint photodynamical and RV model.** Osculating Jacobian orbital parameters valid at BJD=2458743. Time of Conjunction defined in t_{BJD} = 2457000. $\mathcal{N}(\mu, \sigma)$ is normal prior centered at μ with variance of σ; $\mathcal{U}(a, b)$ is uniform prior with lower and upper bounds a, b.

Parameter	Prior	TTV	Photodynamical+RV
Mass Parameters			
Mass ratio, b M_b/M_s ($\times 10^{-5}$)	$\mathcal{U}(0.1, 10)$	$2.2^{+2.0}_{-1.3}$	$2.39^{+0.66}_{-0.64}$
Mass ratio, c M_c/M_s ($\times 10^{-5}$)	$\mathcal{U}(0.1, 10)$	$2.2^{+1.1}_{-1.1}$	$2.58^{+0.50}_{-0.52}$
Mass ratio, d M_d/M_s ($\times 10^{-5}$)	$\mathcal{U}(0.1, 10)$	$4.2^{+2.6}_{-2.3}$	$2.60^{+0.97}_{-0.98}$
Mass ratio, e M_e/M_s ($\times 10^{-5}$)	$\mathcal{U}(0.1, 10)$	-	$1.69^{+0.53}_{-0.53}$
Planet b orbit			
Orbital period P_b (day)	$\mathcal{N}(10.355, 0.1)$	$10.35516^{+0.00032}_{-0.00033}$	$10.35504^{+0.00015}_{-0.00013}$
Eccentricity parameter $e_b \cos\omega_b$	$\mathcal{U}(-0.1, 0.1)$	$0.0058^{+0.0105}_{-0.0052}$	$0.0051^{+0.0049}_{-0.0036}$
Eccentricity parameter $e_b \sin\omega_b$	$\mathcal{U}(-0.1, 0.1)$	$0.0113^{+0.0216}_{-0.0089}$	$0.009^{+0.0061}_{-0.0044}$
Impact parameter b_b	$\mathcal{U}(0, 1)$	-	$0.107^{+0.084}_{-0.072}$
Time of conjunction $T_{\rm conj,b}$ (day)	$\mathcal{N}(1743.7, 0.1)$	$1743.72067^{+0.00091}_{-0.00094}$	$1743.72001^{+0.00086}_{-0.00093}$
Planet c orbit			
Orbital period P_c	$\mathcal{N}(21.014, 0.1)$	$21.0133^{+0.0012}_{-0.0013}$	$21.01447^{+0.00056}_{-0.00063}$
Eccentricity parameter $e_c \cos\omega_c$	$\mathcal{U}(-0.1, 0.1)$	$0.0008^{+0.014}_{-0.0087}$	$-0.0011^{+0.0089}_{-0.0079}$
Eccentricity parameter $e_c \sin\omega_c$	$\mathcal{U}(-0.1, 0.1)$	$0.0004^{+0.0144}_{-0.0094}$	$0.0019^{+0.0095}_{-0.0076}$
Impact parameter b_c	$\mathcal{U}(0, 1)$	-	$0.169^{+0.071}_{-0.089}$
Time of conjunction $T_{\rm conj,c}$	$\mathcal{N}(1748.7, 0.1)$	$1748.69381^{+0.00071}_{-0.00074}$	$1748.69359^{+0.00076}_{-0.00074}$
Planet d orbit			
Orbital period P_d	$\mathcal{N}(35.127, 0.1)$	$35.1279^{+0.0012}_{-0.0011}$	$35.12803^{+0.0006}_{-0.00058}$
Eccentricity parameter $e_d \cos\omega_d$	$\mathcal{U}(-0.1, 0.1)$	$0.0001^{+0.0093}_{-0.0075}$	$0.0011^{+0.0069}_{-0.0058}$
Eccentricity parameter $e_d \sin\omega_d$	$\mathcal{U}(-0.1, 0.1)$	$0.0006^{+0.0112}_{-0.0068}$	$-0.0004^{+0.007}_{-0.0065}$
Impact parameter b_d	$\mathcal{U}(0, 1)$	-	$0.8157^{+0.0069}_{-0.0064}$
Time of conjunction $T_{\rm conj,d}$	$\mathcal{N}(1762.6, 0.1)$	$1762.6669^{+0.0014}_{-0.0014}$	$1762.6667^{+0.0015}_{-0.0015}$
Planet e orbit			
Orbital period P_e	$\mathcal{N}(3.022, 0.1)$	-	$3.0223753^{+8.2e-06}_{-7.7e-06}$
Impact parameter b_e	$\mathcal{U}(0, 1)$	-	$0.102^{+0.086}_{-0.071}$
Time of conjunction $T_{\rm conj,e}$	$\mathcal{N}(1740.2, 0.1)$	-	$1740.21228^{+0.00056}_{-0.00057}$

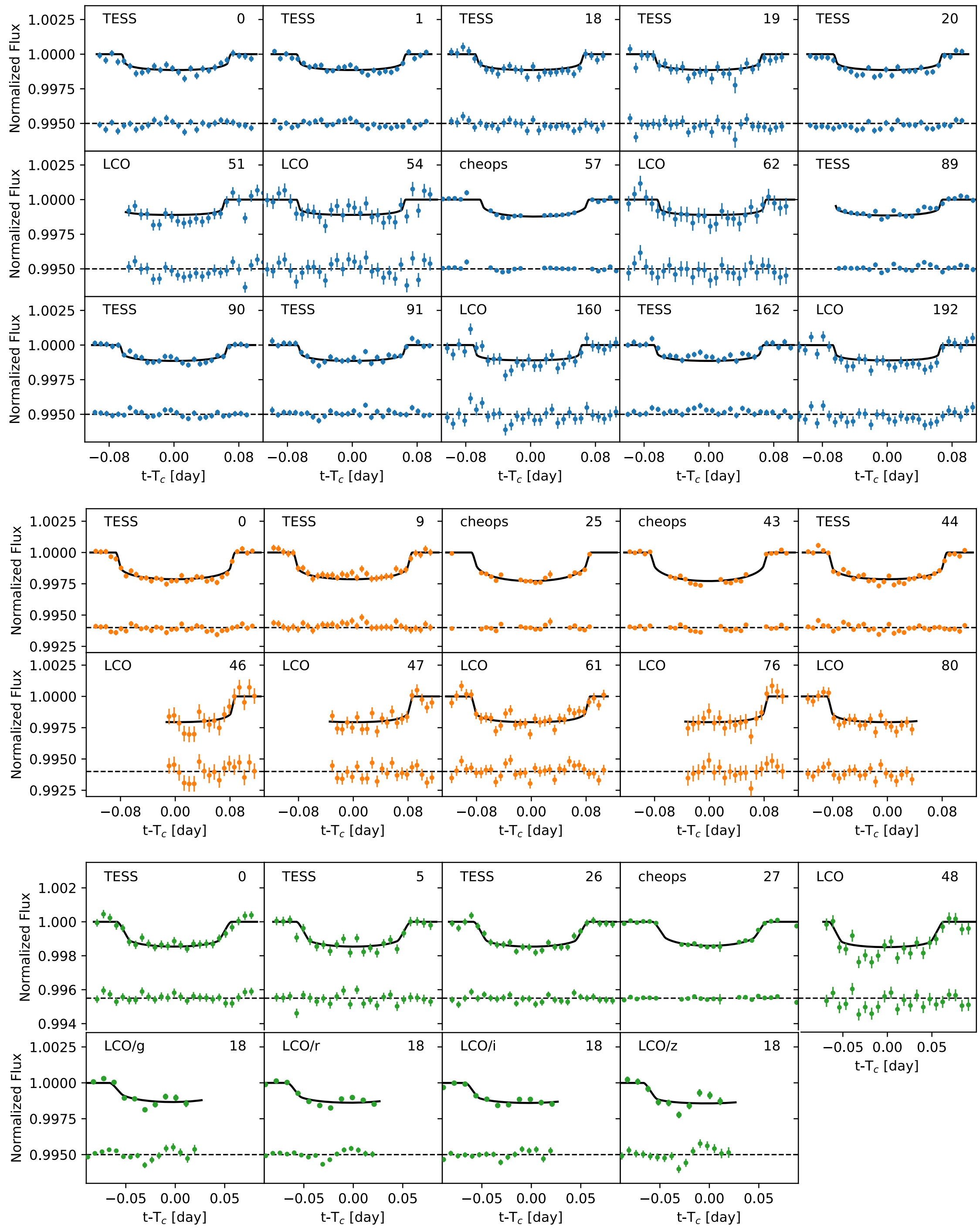

Supplementary Figue 6: **Best-fit photodynamical model for light curves.** The observed transit light curves of TOI-2076 b, c, d are shown in blue, orange and green, respectively. Errorbars are the median and 68% credible interval of photometric data binned to 10-min and shifted to the transit midtimes listed in Table 2. The instruments and transit epoch are shown in the upper part of each panel. The black line is the best-fit photodynamical model. Residuals are plotted in the lower part of the figure.

Supplementary Table 5: **Posterior median and 68.3% (1σ) credible intervals of fitted planetary parameters from the joint photodynamical and RV model.**

Parameter	Prior	Posterior
Stellar parameters		
Stellar radius R_s ($R_\odot$)	$\mathcal{N}(0.758, 0.014)$	$0.7636^{+0.0091}_{-0.0086}$
Stellar mass M_s ($M_\odot$)	$\mathcal{N}(0.849, 0.026)$	$0.842^{+0.024}_{-0.024}$
Planet radii		
Radius ratio, b R_b/R_s	$\mathcal{N}(0.031, 0.005)$	$0.03131^{+0.00025}_{-0.00025}$
Radius ratio, c R_c/R_s	$\mathcal{N}(0.042, 0.005)$	$0.04288^{+0.00031}_{-0.0003}$
Radius ratio, d R_d/R_s	$\mathcal{N}(0.039, 0.005)$	$0.03953^{+0.00038}_{-0.00037}$
Radius ratio, e R_e/R_s	$\mathcal{N}(0.015, 0.005)$	$0.01575^{+0.00035}_{-0.00036}$
RV parameters		
Activity amplitude h_{RV} (m/s)	$\mathcal{J}(0.001, 1000)$	$34.5^{+2.4}_{-2.1}$
Decay timescale τ (day)	$\mathcal{J}(0.001, 1000)$	$26.6^{+1.4}_{-1.3}$
Additive factor Γ	$\mathcal{J}(0.001, 1000)$	$6.1^{+0.72}_{-0.63}$
Rotation period T (day)	$\mathcal{N}(7.34, 0.2)$	$7.338^{+0.012}_{-0.012}$
HIRES RV offset $\gamma_{\rm hires}$ (m/s)	$\mathcal{U}(-50.0, 50.0)$	$0.2^{+4.7}_{-4.6}$
APF RV offset $\gamma_{\rm apf}$ (m/s)	$\mathcal{U}(-50.0, 50.0)$	$-7.2^{+4.9}_{-4.9}$
HARPS RV offset $\gamma_{\rm HARPS}$ (m/s)	$\mathcal{U}(-50.0, 50.0)$	$5.4^{+4.5}_{-4.4}$
HIRES RV jitter noise $\sigma_{\rm hires}$(m/s)	$\mathcal{J}(0.001, 1000)$	$8.1^{+1.4}_{-1.3}$
APF RV jitter noise $\sigma_{\rm apf}$ (m/s)	$\mathcal{J}(0.001, 1000)$	$11.9^{+2.1}_{-1.8}$
HARPS RV jitter noise $\sigma_{\rm HARPS}$(m/s)	$\mathcal{J}(0.001, 1000)$	$4.76^{+0.92}_{-0.91}$
Limb-darkening Coefficients		
$q_{1,\rm TESS}$	$\mathcal{U}(0, 1)$	$0.298^{+0.105}_{-0.088}$
$q_{2,\rm TESS}$	$\mathcal{U}(0, 1)$	$0.47^{+0.14}_{-0.13}$
$q_{1,\rm z}$	$\mathcal{U}(0, 1)$	$0.114^{+0.141}_{-0.081}$
$q_{2,\rm z}$	$\mathcal{U}(0, 1)$	$0.359^{+0.107}_{-0.087}$
$q_{1,\rm CHEOPS}$	$\mathcal{U}(0, 1)$	$0.67^{+0.15}_{-0.13}$
$q_{2,\rm CHEOPS}$	$\mathcal{U}(0, 1)$	$0.31^{+0.18}_{-0.14}$

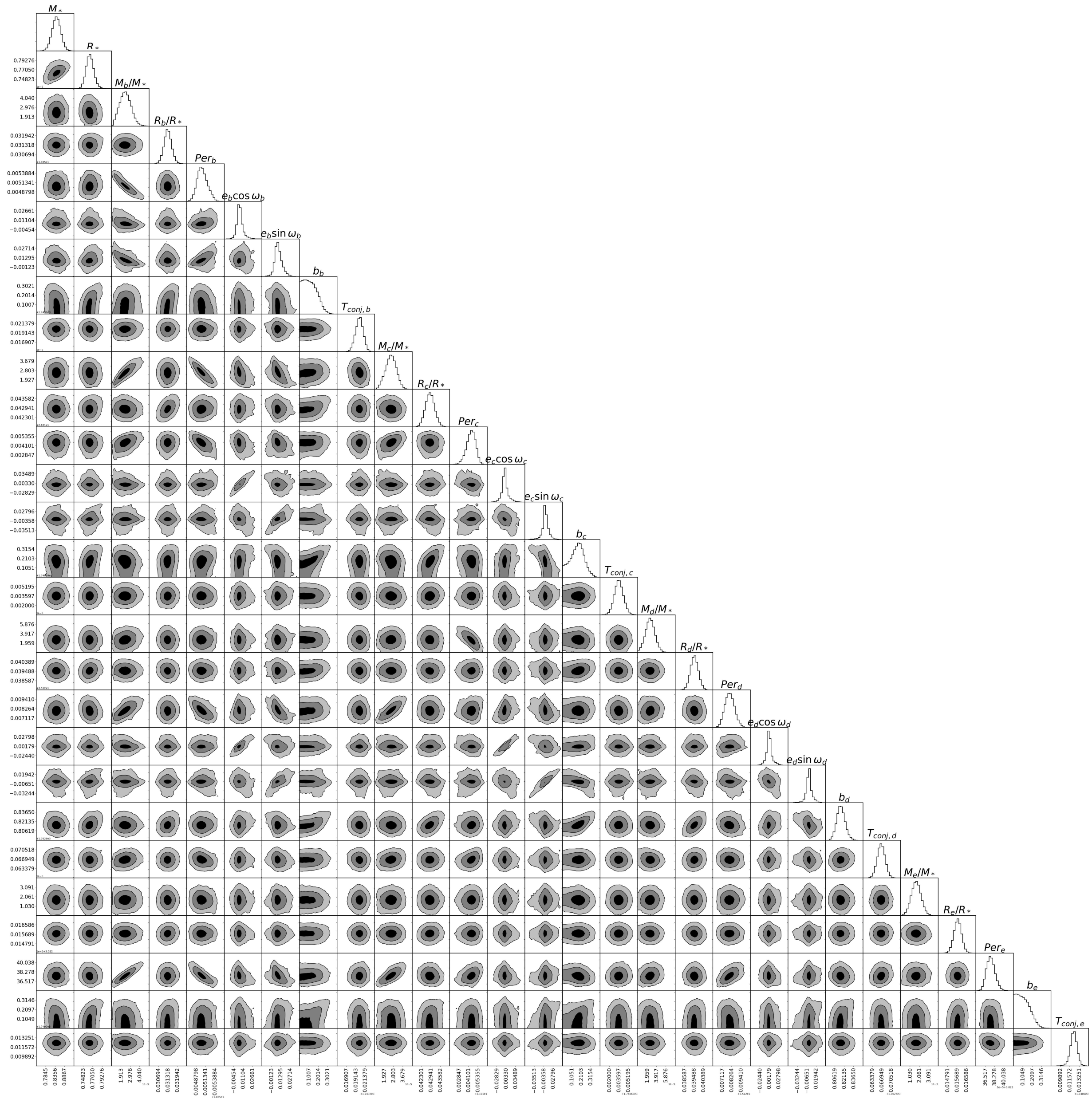

Supplementary Figue 7: **Cornerplots of fitted stellar andplanetary parameters in joint photodynamical+RV model.** The black contours on the 2D panels represent the 1σ, 2σ, and 3σ confidence levels of the overall posterior samples. The diagonal panels show the marginalized probability distribution of each parameter